
19 Sep 2016

Competition between Hydrophilic and Argyrophilic Interactions in Surface Enhanced Raman Spectroscopy

John T. Kelly

Annie K. McClellan

Lynn V. Joe

Ashley M. Wright

et. al. For a complete list of authors, see https://scholarsmine.mst.edu/chem_facwork/3852

Follow this and additional works at: https://scholarsmine.mst.edu/chem_facwork

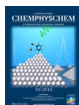
 Part of the [Chemistry Commons](#)

Recommended Citation

J. T. Kelly et al., "Competition between Hydrophilic and Argyrophilic Interactions in Surface Enhanced Raman Spectroscopy," *ChemPhysChem*, pp. 2782 - 2786, Wiley, Sep 2016.

The definitive version is available at <https://doi.org/10.1002/cphc.201600678>

This Article - Journal is brought to you for free and open access by Scholars' Mine. It has been accepted for inclusion in Chemistry Faculty Research & Creative Works by an authorized administrator of Scholars' Mine. This work is protected by U. S. Copyright Law. Unauthorized use including reproduction for redistribution requires the permission of the copyright holder. For more information, please contact scholarsmine@mst.edu.



Competition between Hydrophilic and Argyrophilic Interactions in Surface Enhanced Raman Spectroscopy

John T. Kelly, Annie K. McClellan, Lynn V. Joe, Ashley M. Wright, Lawson T. Lloyd, Gregory S. Tschumper,* and Nathan I. Hammer*^[a]

The competition for binding and charge-transfer (CT) from the nitrogen containing heterocycle pyrimidine to either silver or to water in surface enhanced Raman spectroscopy (SERS) is discussed. The correlation between the shifting observed for vibrational normal modes and CT is analyzed both experimentally using Raman spectroscopy and theoretically using electronic structure theory. Discrete features in the Raman spectrum correspond to the binding of either water or silver to each of pyrimidine's nitrogen atoms with comparable frequency shifts. Natural bond orbital (NBO) calculations in each chemical environment reveal that the magnitude of charge transfer from pyrimidine to adjacent silver atoms is only about twice that for water alone. These results suggest that the choice of solvent plays a role in determining the vibrational frequencies of nitrogen containing molecules in SERS experiments.

Although the exact mechanism is not fully understood, Fleischmann et al. made a lasting impression in the scientific community with the spectroscopic observation of "physisorbed" pyridine on a silver surface nearly half of a century ago.^[1] Today, surface-enhanced Raman spectroscopy (SERS) is employed in a wide range of applications to characterize both inter- and intramolecular interactions.^[2–11] Many biologically relevant molecules have weak Raman scattering and/or exhibit problematic fluorescence, making structural assignment difficult.^[12] SERS helps facilitate the detection and analysis of such molecules by increasing the scattering intensity on the order of 10^6 times,^[13–16] and this enhancement makes SERS a powerful analytical technique. Despite all the progress, the contributions from electromagnetic (EM) and charge-transfer (CT) enhancements to the SERS effect continues to be debated.^[13,17–20]

The nitrogen-containing heterocycle pyridine is one of the most studied SERS-active molecules, and its vibrational spectrum is still examined today both experimentally and theoretically in efforts to better understand the fundamental molecular interactions that give rise to this nascent enhancement.^[21–25]

Fleischmann et al. even suggested in their 1974 work the importance of the orientation of the water molecules to the SERS phenomenon.^[1] Here, in order to study the interactions of a nitrogen containing heterocycle with silver and water, we choose to study the two-nitrogen-atom analogue pyrimidine. Pyrimidine is a more biologically relevant building block and offers two potential binding sites to silver and water. Previously, we employed a combination of Raman spectroscopy and electronic structure computations to correlate partial CT from pyrimidine to extended hydrogen-bonded solvent networks to shifts in the Raman spectrum of pyrimidine.^[26–28] In those studies, we considered eight different solvent molecules and over 100 microsolvated molecular clusters to establish a direct correlation between the magnitude of charge transfer and the resulting frequency shifts. Such shifts are common in SERS spectra and also likely originate from partial charge transfer.^[29–31]

Centeno et al. previously investigated the SERS spectra of nitrogen-containing heterocycles, including pyrimidine in aqueous solutions.^[32,33] These authors noted shifts in the Raman spectra of the nitrogen-containing heterocycles in these solutions and compared their experimental results to the results of electronic structure calculations. They focused their analysis on the interactions between metal electrodes and the absorbate and quantified the SERS enhancements. Here, in order to separate the contributions of CT from pyrimidine to silver and pyrimidine to the hydrogen-bonded water network, we compare, for the first time, the Raman spectra of solvated pyrimidine (Pm/H₂O) to the SERS spectra of both neat pyrimidine on silver substrate (Pm/Ag) and pyrimidine on silver substrate in the presence of water (Pm/H₂O/Ag), both experimentally and theoretically. We also compare these results to our earlier studies.

Figure 1 compares the experimental Raman spectra of pure pyrimidine (Figure 1 a) with that of a 1 M pyrimidine/water mixture (Figure 1 b) as well as the SERS spectra of pure pyrimidine on a silver island film (Figure 1 c) with that of a 1 M pyrimidine/water mixture on a silver island film (Figure 1 d). Water's bending and stretching modes are apparent in the aqueous pyrimidine/water mixture in Figure 1 a. Details of the experimental techniques are included in the Supporting Information. Certain vibrational normal modes of pyrimidine are observed to either blue-shift (shift to higher energy) or red-shift (shift to lower energy) in the presence of water, by up to 14 cm^{-1} . Similar shifts are observed in the SERS spectra of both pyrimidine and the pyrimidine/water mixture when absorbed to a silver substrate. These vibrational energy level shifts are tabulated in Table 1. In our earlier works we analyzed our experimental results with the use of Natural Bond Orbital (NBO) analyses and

[a] J. T. Kelly, A. K. McClellan, L. V. Joe, A. M. Wright, L. T. Lloyd, Prof. G. S. Tschumper, Prof. N. I. Hammer
Department of Chemistry and Biochemistry
University of Mississippi, P.O. Box 1848, University, Mississippi 38677 (United States)
E-mail: tschumpr@olemiss.edu
nhammer@olemiss.edu

Supporting Information and the ORCID identification number(s) for the author(s) of this article can be found under <http://dx.doi.org/10.1002/cphc.201600678>.

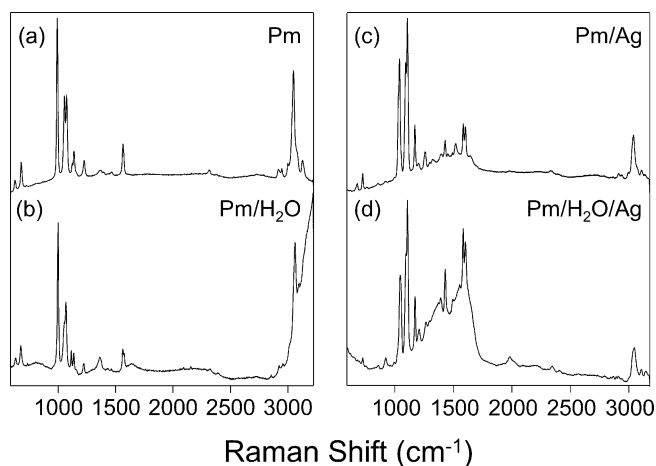


Figure 1. Raman spectra of a) neat pyrimidine, b) a 1 M aqueous pyrimidine solution, and SERS spectra of c) neat pyrimidine and d) a 1 M aqueous pyrimidine solution.

Symmetry	Mode	Pm ν	Pm/H ₂ O $\Delta\nu$	Pm/Ag $\Delta\nu$	Pm/H ₂ O/Ag $\Delta\nu$
A ₁	ν_{6a}	681	+5	+3	–
	ν_1	990	+14	+13/+25	+14
	ν_{9a}	1139	+5	–1	+1
	ν_{8a}	1564	+6	–4	–4
B ₂	ν_3	1228	+3	+6	+5
	ν_{8b}	1571	+12	+7/+11	+9

attributed this blue-shifting to result from electron density transfer from pyrimidine's lone pairs to the hydrogen-bonded network.^[26–27] Here, we apply this same computational approach to study interactions with the silver substrate.

Both Raman and SERS spectra of pyrimidine include a prominent feature at 990 cm^{-1} (ν_1), which is the pyrimidine's ring breathing mode. This mode is common to all benzene-like molecules and exhibits the largest change in polarizability upon excitation and therefore the largest Raman cross-section. A high resolution comparison of this region is shown in Figure 2. We,^[27–28] and others,^[34–36] previously showed in the cases of pyrimidine interacting with water, methanol, and ethylene glycol, that the features labeled here by α , β , and γ originate from interactions with 0, 1, and 2 hydrogen-bonded groups, respectively. In the cases with water, these features are broader due to the many possible hydrogen-bonded geometries. With methanol (see Figure S1), however, these features are more distinct and similar to the case of Figure 2c, suggesting that, in addition to free pyrimidine molecules (α), pyrimidine molecules also exhibit interactions with silver by both one (β) or both nitrogen atoms (γ). The differences in the ratios of the features α , β , and γ in Figures 2c,d suggest that both water and silver are interacting with pyrimidine.

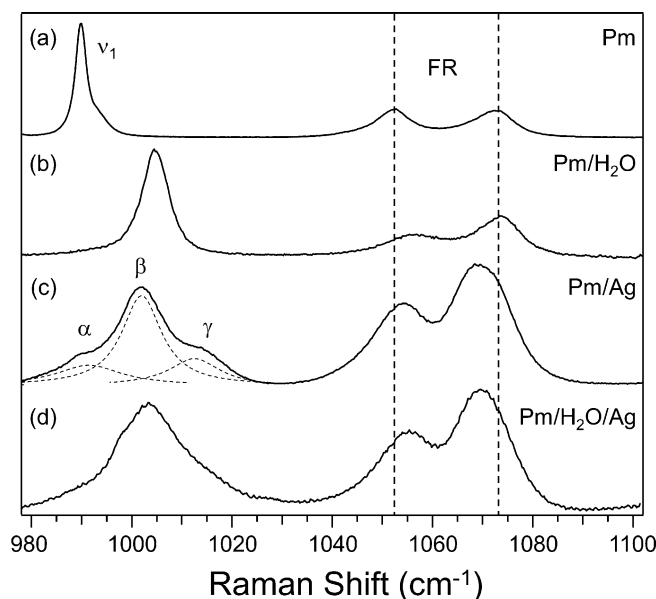


Figure 2. Higher-resolution Raman and SERS spectra of pyrimidine and aqueous pyrimidine solutions in the region of pyrimidine's ring breathing mode ν_1 and Fermi resonance (FR). Peaks labeled by α , β , and γ indicate 0, 1, or 2, respectively, interactions with silver and the Lorentzian fits in (c) indicate contributions from three distinct binding motifs.

Also in this region, centered at 1060 cm^{-1} , are two peaks that are equal in intensity in the Raman spectrum of pure pyrimidine. This feature has been assigned by different authors as a Fermi resonance (FR) including ν_{12} and a combination band, most usually $\nu_{10b} + \nu_{16b}$, although the actual assignment is still debated in the literature. We previously showed that ν_{16b} (centered at 351 cm^{-1} in pure pyrimidine) exhibits a shift of $+2\text{ cm}^{-1}$ in the presence of water. Interestingly, in the cases of pyrimidine interacting with only water, only silver, and silver and water together, these peaks get closer together and their relative intensities change, indicating that the overlap in the energies of these modes is no longer favorable.

Figure 3 shows higher-resolution spectra of the symmetric and asymmetric ring-stretching modes of pyrimidine, ν_{8a} and ν_{8b} , respectively, near 1560 cm^{-1} . In the SERS spectra of pyrimidine, there is also a substantial enhancement of these features. This is especially true in aqueous solution as shown in Figure 1c. As in the case of ν_1 , multiple spectral components are apparent in ν_{8b} when pyrimidine interacts with silver, suggesting that binding by silver to either one or two nitrogen atoms yields different vibrational energy shifts. However, it is also apparent from the smaller blue shift in Figure 3d that water effectively competes with silver for binding with pyrimidine.

Centeno et al. previously suggested that the increase in Raman activity of ν_{8a} and ν_{8b} has its origins in resonance Raman effects, Herzberg–Teller intensity borrowing, and Frank–Condon factor enhancements.^[37] It is important to point out that this effect is more pronounced in the presence of water (Figure 1c vs. Figure 1d), suggesting that the solvent is playing an important role in this enhancement.

Harmonic vibrational frequencies of silver clusters interacting with organic molecules have previously been computed using

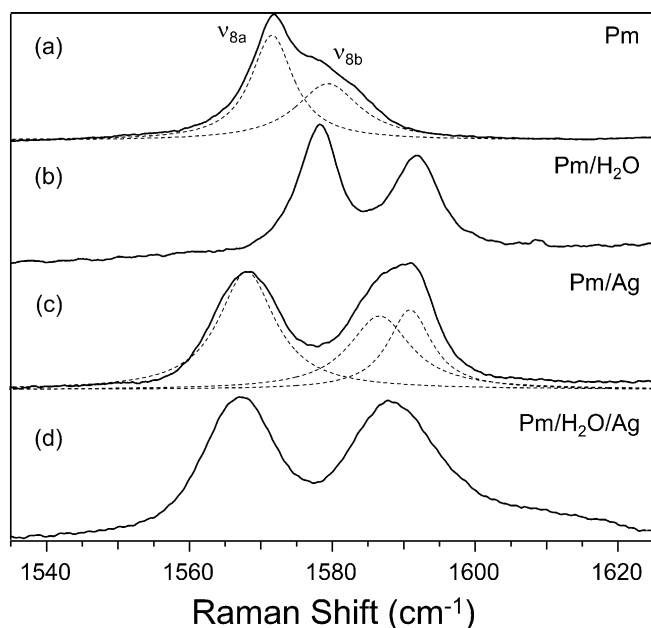


Figure 3. Higher-resolution Raman and SERS spectra of pyrimidine and aqueous pyrimidine solutions showing the symmetric and asymmetric ring-stretching modes ν_{8a} and ν_{8b} , respectively.

a variety of density functional theory (DFT) methods^[38–39] with different basis sets.^[32,40] Here, Becke's three-parameter exchange functional with the Lee–Yang–Parr correlation^[41–42] is employed with several basis sets in an attempt to accurately describe charge transfer between silver clusters, solute, and water. Full geometry optimizations and frequency analyses were performed using the B3LYP hybrid density functional along with suitable triple- ζ basis sets and the Gaussian09 software package.^[43] For comparison, calculations were also performed using the M06-2X^[44] and M06-L^[45] functionals and results are included in the Supporting Information. Figure 4 shows optimized molecule cluster geometries for pyrimidine interacting with either water, Ag_2 , or water and Ag_2 . Although the number of silver atoms for a given nanocluster is known to affect the structure and resulting vibrational frequencies in nitrogen-containing molecules, Schatz showed that this varia-

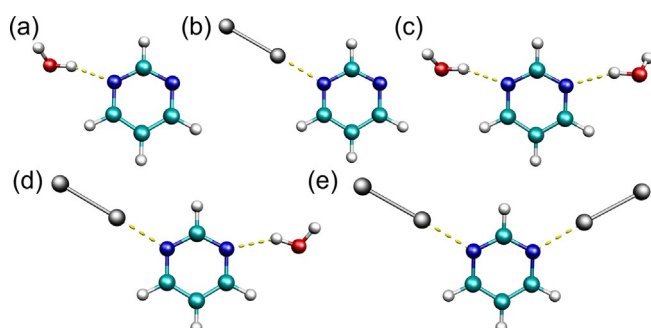


Figure 4. Optimized minimum energy geometries of a) pyrimidine hydrogen-bonded to one water molecule, b) pyrimidine interacting with a silver dimer, c) pyrimidine hydrogen-bonded to two water molecules, d) pyrimidine interacting with both a silver dimer and a water molecule, and e) pyrimidine interacting with two silver dimers.

tion is relatively small and also depends on the placement of the silver atoms.^[46] Here we explore the interactions between pyrimidine and silver using Ag_2 because the deviation expected from choice of the number of silver atoms is less than the absolute error expected from the choice of the level of theory, and this selection allows a convenient comparison with interactions with water.

We previously showed that symmetrically solvated pyrimidine clusters reproduced experimental shifts in the cases of water, methanol, and other hydrogen-bonded solvents.^[26–28] In each of these cases, these weakly interacting complexes, including the structure shown in Figure 4c, are energetically more stable than the individual monomers. Each complex is bound by at least $10.6 \text{ kcal mol}^{-1}$ according to B3LYP computations with the Dunning correlation-consistent aug-cc-pVTZ basis set with a pseudopotential for silver atoms (hereafter denoted aTZ-PP). For the $\text{H}_2\text{O}\cdots\text{Pm}\cdots\text{H}_2\text{O}$ structure shown in Figure 4c, the computed interaction energy is $10.6 \text{ kcal mol}^{-1}$, but this value nearly doubles to $20.8 \text{ kcal mol}^{-1}$ for the corresponding $\text{Ag}_2\cdots\text{Pm}\cdots\text{Ag}_2$ structure in Figure 4e.

Tables 2 and 3 compare the observed Raman shifts with those from harmonic vibrational frequencies for the B3LYP/aTZ-PP structures in Figure 3. Results with other functionals and basis sets are included in the Supporting Information. The agreement between theory and experiment for pyrimidine interacting with silver is good. This is especially true for the spectral features β and γ in Figure 2c, which are experimentally $+13$ and $+25 \text{ cm}^{-1}$, respectively. These agree well with the

Table 2. Comparison of the experimental (Pm/ H_2O) and the computed (Pm $\cdots\text{H}_2\text{O}$ and $\text{H}_2\text{O}\cdots\text{Pm}\cdots\text{H}_2\text{O}$) vibrational energy shifts [cm^{-1}] of certain normal modes of pyrimidine when interacting with water using the B3LYP method and the aug-cc-pVTZ basis set.

Mode		Pm/ H_2O	Pm $\cdots\text{H}_2\text{O}$	$\text{H}_2\text{O}\cdots\text{Pm}\cdots\text{H}_2\text{O}$
A_1	ν_{6a}	+5	+4	+7
	ν_1	+14	+8	+15
	ν_{9a}	+5	+2	+4
	ν_{8a}	+6	−1	+3
B_2	ν_3	+3	+4	+9
	ν_{8b}	+12	+9	+11

Table 3. Comparison of the experimental (Pm/ Ag and Pm/ $\text{H}_2\text{O}/\text{Ag}$) and the computed (Pm $\cdots\text{Ag}_2$, $\text{Ag}_2\cdots\text{Pm}\cdots\text{Ag}_2$, and $\text{H}_2\text{O}\cdots\text{Pm}\cdots\text{Ag}_2$) vibrational energy shifts [cm^{-1}] of certain normal modes of pyrimidine when interacting with silver and water and silver using the B3LYP method and the aug-cc-pVTZ basis set.

Mode		Pm/ Ag	Pm $\cdots\text{Ag}_2$	$\text{Ag}_2\cdots\text{Pm}\cdots\text{Ag}_2$	Pm/ $\text{H}_2\text{O}/\text{Ag}$	$\text{H}_2\text{O}\cdots\text{Pm}\cdots\text{Ag}_2$
A_1	ν_{6a}	+3	+2	−4	−	+4
	ν_1	+13/ +25	+13	+22	+13	+19
	ν_{9a}	−1	−1	−6	+1	+2
B_2	ν_{8a}	−4	−4	+5	−4	−1
	ν_3	+6	+4	+15	+5	+9
	ν_{8b}	+7/ +11	+14	+20	+9	+15

computed values of +13 and +22 cm⁻¹ for binding by silver to either one or both of pyrimidine's nitrogen atoms.

The NBO results shown in Table 4 suggest partial electron transfer from the pyrimidine to both adjacent water molecules

Table 4. NBO analysis comparing partial charge transfer [me⁻] from pyrimidine to water molecules and/or silver atoms.

	Pm	H ₂ O	Ag ₂
Pm...H ₂ O	22.4	-22.4	-
H ₂ O...Pm...H ₂ O	40.4	-20.2	-
Pm...Ag ₂	79.3	-	-79.2
Ag ₂ ...Pm...Ag ₂	145.2	-	-72.6
H ₂ O...Pm...Ag ₂	90.2	-13.5	-76.6

and the silver island films.^[47] This CT is the origin of the spectral blue shifts in a number of normal modes in pyrimidine. The analysis of these results quantifies for the first time the magnitude at which partial charge transfer plays a role in this widely applied technique in competition with the solvent, in this case water. Although charge transfer to silver dominates, consideration of the solvent, especially water, should not be neglected. Over 10% of the charge transfer is distributed to the hydrogen bound water molecule when both silver and water are interacting at the same time with pyrimidine. This number is likely much larger than 10% in aqueous solution since Δq increases with the number of water molecules hydrogen bonded to the complex.^[26-27]

In summary, we demonstrate that the interactions of the nitrogen-containing building block pyrimidine with either silver or water are remarkably similar in terms of blue-shifted vibrational frequencies and partial CT. We also demonstrate that the agreement between experiment and theory is very good in these systems. Although the binding of pyrimidine to silver is preferential to that with water, binding with water still competes as evidenced by differences in the SERS spectra of ν_1 and pyrimidine's Fermi resonance near 1060 cm⁻¹. In a pyrimidine cluster with a single water molecule and a single Ag₂ moiety, H₂O accepts more than 10% of the charge being transferred from pyrimidine to its neighbors according to NBO analyses. Together, these results suggest that interactions with both silver and water account for the spectral features observed experimentally in SERS experiments and that the choice of solvent in SERS likely plays an important role in the observed vibrational spectra of nitrogen containing heterocyclic molecules.

Acknowledgements

This material is based on work supported by the National Science Foundation under Grant Nos. EPS-0903787, CHE-0955550, CHE-1156713, CHE-1338056, and CHE-1532079.

Keywords: charge transfer • NBO analysis • Raman spectroscopy • SERS • silver island films

- [1] M. Fleischmann, P. J. Hendra, A. J. McQuillan, *Chem. Phys. Lett.* **1974**, *26*, 163–166.
- [2] R. Maher, C. Galloway, E. Le Ru, L. Cohen, P. Etchegoin, *Chem. Soc. Rev.* **2008**, *37*, 965–979.
- [3] M. D. Porter, R. J. Lipert, L. M. Siperko, G. Wang, R. Narayanan, *Chem. Soc. Rev.* **2008**, *37*, 1001–1011.
- [4] W. Smith, *Chem. Soc. Rev.* **2008**, *37*, 955–964.
- [5] Y. S. Huh, A. J. Chung, D. Erickson, *Microfluid. Nanofluid.* **2009**, *6*, 285–297.
- [6] K. S. Joya, X. Sala, *Phys. Chem. Chem. Phys.* **2015**, *17*, 21094–21103.
- [7] K. Kneipp, Y. Wang, H. Kneipp, L. T. Perelman, I. Itzkan, R. R. Dasari, M. S. Feld, *Phys. Rev. Lett.* **1997**, *78*, 1667.
- [8] S. Nie, S. R. Emory, *Science* **1997**, *275*, 1102–1106.
- [9] D. Radziuk, H. Moehwald, *Phys. Chem. Chem. Phys.* **2015**, *17*, 21072–21093.
- [10] E. Le Ru, P. Etchegoin, *Principles of Surface-Enhanced Raman Spectroscopy and Related Plasmonic Effects*, Elsevier, Amsterdam, **2008**.
- [11] Y. Wang, Z. Yu, W. Ji, Y. Tanaka, H. Sui, B. Zhao, Y. Ozaki, *Angew. Chem. Int. Ed.* **2014**, *53*, 13866–13870; *Angew. Chem.* **2014**, *126*, 14086–14090.
- [12] A. Campion, P. Kambhampati, *Chem. Soc. Rev.* **1998**, *27*, 241–250.
- [13] M. Moskovits, *Rev. Mod. Phys.* **1985**, *57*, 783–826.
- [14] J. E. Rowe, C. V. Shank, D. A. Zwemer, C. A. Murray, *Phys. Rev. Lett.* **1980**, *44*, 1770–1773.
- [15] S. S. R. Dasary, A. K. Singh, D. Senapati, H. Yu, P. C. Ray, *J. Am. Chem. Soc.* **2009**, *131*, 13806–13812.
- [16] V. S. Tiwari, T. Oleg, G. K. Darbha, W. Hardy, J. Singh, P. C. Ray, *Chem. Phys. Lett.* **2007**, *446*, 77–82.
- [17] J. R. Lombardi, R. L. Birke, T. Lu, J. Xu, *J. Chem. Phys.* **1986**, *84*, 4174–4180.
- [18] M. Osawa, N. Matsuda, K. Yoshii, I. Uchida, *J. Phys. Chem.* **1994**, *98*, 12702–12707.
- [19] H. Yamada, H. Nagata, K. Toba, Y. Nakao, *Surf. Sci.* **1987**, *182*, 269–286.
- [20] Y. Fang, N.-H. Seong, D. D. Dlott, *Science* **2008**, *321*, 388–392.
- [21] L. Chen, Y. Gao, H. Xu, Z. Wang, Z. Li, R.-Q. Zhang, *Phys. Chem. Chem. Phys.* **2014**, *16*, 20665–20671.
- [22] X.-k. Kong, Q.-w. Chen, Z. -y. Sun, *Chem. Phys. Lett.* **2013**, *564*, 54–59.
- [23] J.-F. Li, Y.-J. Zhang, A. V. Rudnev, J. R. Anema, S.-B. Li, W.-J. Hong, P. Rajapandian, J. Lipkowski, T. Wandlowski, Z.-Q. Tian, *J. Am. Chem. Soc.* **2015**, *137*, 2400–2408.
- [24] D.-Y. Wu, X.-M. Liu, S. Duan, X. Xu, B. Ren, S.-H. Lin, Z.-Q. Tian, *J. Phys. Chem. C* **2008**, *112*, 4195–4204.
- [25] L. Zhao, L. Jensen, G. C. Schatz, *J. Am. Chem. Soc.* **2006**, *128*, 2911–2919.
- [26] A. A. Howard, G. S. Tschumper, N. I. Hammer, *J. Phys. Chem. A* **2010**, *114*, 6803–6810.
- [27] A. M. Wright, A. A. Howard, J. C. Howard, G. S. Tschumper, N. I. Hammer, *J. Phys. Chem. A* **2013**, *117*, 5435–5446.
- [28] J. C. Howard, N. I. Hammer, G. S. Tschumper, *ChemPhysChem* **2011**, *12*, 3262–3273.
- [29] E. Hesse, J. Creighton, *Langmuir* **1999**, *15*, 3545–3550.
- [30] A. M. Fales, H. Yuan, T. Vo-Dinh, *Langmuir* **2011**, *27*, 12186–12190.
- [31] J. Suh, M. Moskovits, *J. Am. Chem. Soc.* **1986**, *108*, 4711–4718.
- [32] S. P. Centeno, I. Lopez-Tocon, J. F. Arenas, J. Soto, J. C. Otero, *J. Phys. Chem. B* **2006**, *110*, 14916–14922.
- [33] S. P. Centeno, I. Lopez-Tocon, J. Roman-Perez, J. F. Arenas, J. Soto, J. C. Otero, *J. Phys. Chem. C* **2012**, *116*, 23639–23645.
- [34] H. Takahashi, K. Mamola, E. K. Plyler, *J. Mol. Spectrosc.* **1966**, *21*, 217–230.
- [35] S. Schlücker, J. Koster, R. K. Singh, B. P. Asthana, *J. Phys. Chem. A* **2007**, *111*, 5185–5191.
- [36] D. K. Singh, S. Mishra, A. K. Ojha, S. K. Srivastava, S. Schlücker, B. P. Asthana, J. Popp, R. K. Singh, *J. Raman Spectrosc.* **2011**, *42*, 667–675.
- [37] J. F. Arenas, M. S. Woolley, I. L. Tocón, J. C. Otero, J. I. Marcos, *J. Chem. Phys.* **2000**, *112*, 7669–7683.
- [38] S. Barsberg, *Theor. Chem. Acc.* **2015**, *134*, 1–12.
- [39] M. Pagliai, L. Bellucci, M. Muniz-Miranda, G. Cardini, V. Schettino, *Phys. Chem. Chem. Phys.* **2006**, *8*, 171–178.
- [40] C. M. Aikens, G. C. Schatz, *J. Phys. Chem. A* **2006**, *110*, 13317–13324.
- [41] A. D. Becke, *Phys. Rev. A* **1988**, *38*, 3098–3100.
- [42] C. Lee, W. Yang, R. G. Parr, *Phys. Rev. B* **1988**, *37*, 785–789.

- [43] Gaussian09, Revision D.01 M. J. Frisch, G. W. Trucks, H. B. Schlegel, G. E. Scuseria, M. A. Robb, J. R. Cheeseman, G. Scalmani, V. Barone, B. Menucci, G. A. Petersson, H. Nakatsuji, M. Caricato, X. Li, H. P. Hratchian, A. F. Izmaylov, J. Bloino, G. Zheng, J. L. Sonnenberg, M. Hada, M. Ehara, K. Toyota, R. Fukuda, J. Hasegawa, M. Ishida, T. Nakajima, Y. Honda, O. Kitao, H. Nakai, T. Vreven, J. A. Montgomery, Jr., J. E. Peralta, F. Ogliaro, M. J. Bearpark, J. Heyd, E. N. Brothers, K. N. Kudin, V. N. Staroverov, R. Kobayashi, J. Normand, K. Raghavachari, A. P. Rendell, J. C. Burant, S. S. Iyengar, J. Tomasi, M. Cossi, N. Rega, N. J. Millam, M. Klene, J. E. Knox, J. B. Cross, V. Bakken, C. Adamo, J. Jaramillo, R. Gomperts, R. E. Stratmann, O. Yazyev, A. J. Austin, R. Cammi, C. Pomelli, J. W. Ochterski, R. L. Martin, K. Morokuma, V. G. Zakrzewski, G. A. Voth, P. Salvador, J. J. Dannenberg, S. Dapprich, A. D. Daniels, Ö. Farkas, J. B. Foresman, J. V. Ortiz, J. Cioslowski, D. J. Fox, Gaussian, Inc., Wallingford, CT, USA, **2009**.
- [44] Y. Zhao, D. G. Truhlar, *Theo. Chem. Acc.* **2008**, *120*, 215–241.
- [45] Y. Zhao, D. G. Truhlar, *J. Chem. Phys.* **2006**, *125*, 194101.
- [46] L. Jensen, L. L. Zhao, G. C. Schatz, *J. Phys. Chem. C* **2007**, *111*, 4756–4764.
- [47] R. Van Duyne, J. Hultheen, D. Treichel, *J. Chem. Phys.* **1993**, *99*, 2101–2115.

Manuscript received: June 23, 2016
Accepted Article published: June 28, 2016
Final Article published: July 7, 2016